

# Electroproduction of medium- and heavy-mass hypernuclei

Petr Bydžovský,

Daria Denisova, Dimitrios Petrellis, Dalibor Skoupil, and Petr Veselý

Outline:

## Introduction

### Formalism of DWIA

- impulse approximation in optimal factorisation,
- elementary amplitude in a general two-component form
- optimum on-shell approximation

### Results: effects in the cross sections from

- kinematics (Fermi motion, the mass),
- kaon distortion,
- $\Lambda N$  interaction.

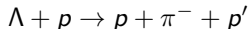
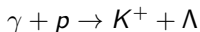
Predictions for the JLab experiments on  ${}^{40}_{\Lambda}\text{Ca}$ ,  ${}^{48}_{\Lambda}\text{Ca}$ , and  ${}^{208}_{\Lambda}\text{Pb}$ .

## Summary

More information in Phys. Rev. C **106**, 044609 (2022) and **108**, 024615 (2023).

# Introduction – Why and how to study hypernuclei?

- a direct investigation of the **YN interaction** is quite complicated, e.g.  $\Lambda p$  scattering in the liquid-hydrogen target



[see J. Rowley et al (CLAS Collaboration), Phys. Rev. Lett. 127, 272303 (2021)], information on the bare YN interaction is limited (Nijmegen model)

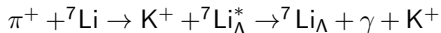
- the  $\gamma$ -ray and **reaction spectroscopy** of  $\Lambda$  hypernuclei can provide information on the **spin-dependent part** of an effective  $\Lambda N$  interaction

$$V_{\Lambda N} = V_0 + V_\sigma \vec{s}_\Lambda \cdot \vec{s}_N + V_\Lambda \vec{\ell}_{\Lambda N} \cdot \vec{s}_\Lambda + V_N \vec{\ell}_{\Lambda N} \cdot \vec{s}_N + V_T S_{12}$$

- in hypernuclei one can study  $\Lambda$ - $\Sigma$  mixing:  $\Lambda + N \longleftrightarrow \Sigma^0 + N$ ;  
charge symmetry breaking in mirror hypernuclei:  ${}^4_\Lambda\text{He} - {}^4_\Lambda\text{H}$ ,  ${}^{16}_\Lambda\text{N} - {}^{16}_\Lambda\text{O}$ ;  
and non mesonic weak decays of  $\Lambda$ :  $\Lambda N \longrightarrow nN$

# Introduction – the $\gamma$ -ray (classical) spectroscopy

- an example of  $\gamma$ -ray transitions in the hadron-induced reaction

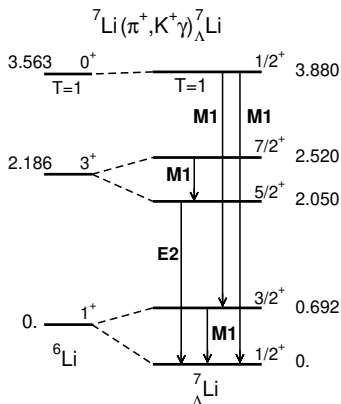


with  $\text{K}^+$  and  $\gamma$  detected in coincidence

- $\gamma$ 's are measured by Ge detector array with a high resolution  $\approx 1$  keV
- analysis of spectra was done for p-shell hypernuclei  $\rightarrow$  the effective interaction  $V_{\Lambda N}$  was obtained [D. J. Millener, Nucl.Phys. A 804, 84 (2008)]

- limitations:
  - only the low-lying states are determined (below the particle emission threshold)
  - the ground-state binding energy cannot be determined

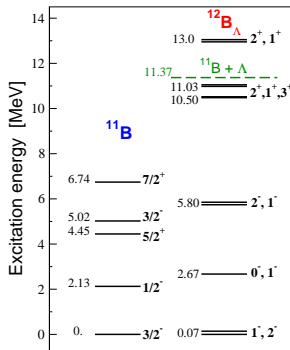
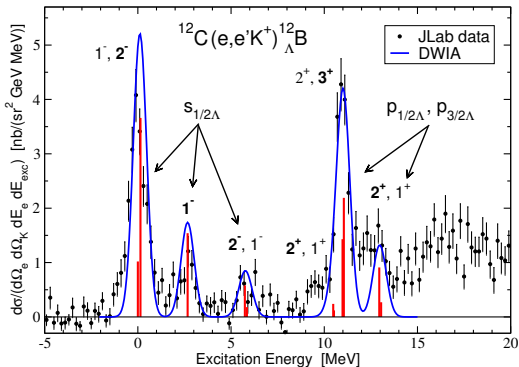
*$\Lambda$  hypernucleus is a relatively long living system  $\approx 10^{-10}$  s*



by H. Tamura

# Introduction – the reaction spectroscopy

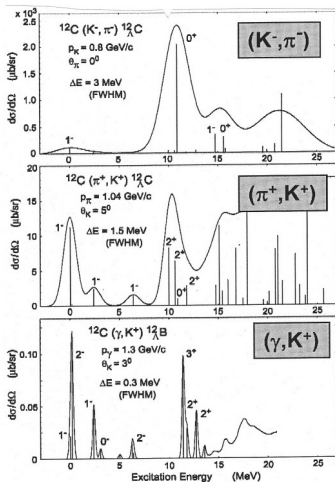
- the reaction spectroscopy allows to study also the high-excited states e.g. here those with  $\Lambda$  in the  $p$  orbit
- missing mass spectrum in  $e + {}^{12}\text{C} \rightarrow e' + K^+ + {}^{12}\text{B}_\Lambda^*$ , where  $e'$  and  $K^+$  are detected
- the energy resolution is worse than in the  $\gamma$  spectroscopy but below 1 MeV



M. Iodice et al, Phys. Rev. Lett. **99**, 052501 (2007)

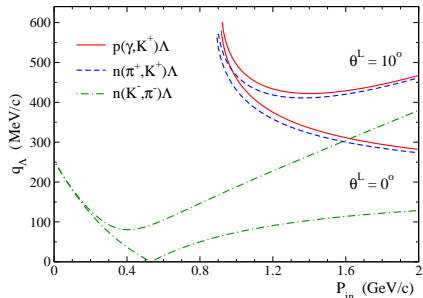
# Introduction – electroproduction of hypernuclei

- one can achieve a better energy resolution than in the  $\pi^+$  and  $K^-$  induced reactions



by Hashimoto and Tamura

- large momentum transfer:  $q_{\Lambda} > 250 \text{ MeV}/c$



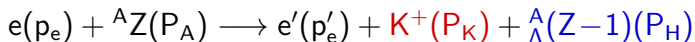
- one can also study the **reaction mechanism**:  
 kinematical effects, factorization, off-shell effects, kaon distortion,...; and test the elementary amplitudes

# Introduction – electroproduction of hypernuclei

- other characteristics of electroproduction:
  - the electro-magnetic interaction is well known and weak ( $\alpha \approx 1/137$ )
    - the **one-photon exchange approximation** is very good which simplifies description to production by virtual photons:  $A(\gamma_\nu, K^+)H$
  - production is on the proton
    - other hypernuclei than in  $(\pi^+, K^+)$  and  $(K^-, \pi^-)$  reactions
  - if  $K^0$  is detected then production goes on the neutron in  $(\gamma, K^0)$
  - a strong **spin-flip** → the highest-spin states in multiplets dominate
- typical kinematics in experiments:
  - a small electron scattering angle and **small photon virtuality**  $Q^2 = -q^2$ 
    - this is to achieve sufficiently big virtual photon flux ( $\Gamma$ ),
  - kaon is detected along the photon direction (z-axis) at a **very small kaon angle** ( $\theta_K$ )
- To obtain reliable information from hypernucleus electroproduction data we need to understand the reaction mechanism well, e.g. to estimate systematic uncertainties due to various approximations.

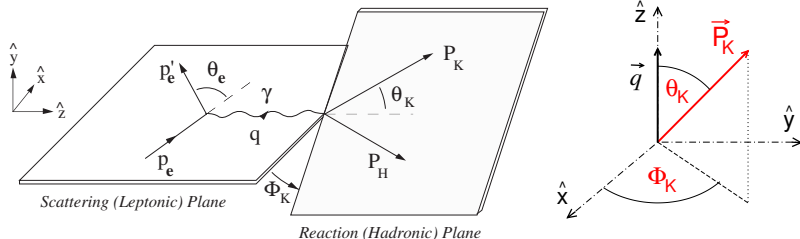
# Formalism – kinematics in electroproduction

- production on the proton:



photon energy and momentum:  $E_\gamma = E_e - E'_e$  and  $\vec{q} = \vec{p}_e - \vec{p}'_e$

- in the laboratory frame ( $\vec{P}_A = 0$ ):



- kinematics in an experiment:  $E_e, E'_e, \theta_e, \theta_{K_e}, \Phi_K$

$\rightarrow \epsilon, \Gamma, q = p_e - p'_e, Q^2 = -q^2, |\vec{P}_K|, \theta_K \dots$

# Formalism – the cross section

- the unpolarized triple-differential cross section

$$\frac{d^3\sigma}{dE'_e d\Omega'_e d\Omega_K} = \Gamma \left[ \frac{d\sigma_T}{d\Omega_K} + \epsilon_L \frac{d\sigma_L}{d\Omega_K} + \epsilon \frac{d\sigma_{TT}}{d\Omega_K} + \sqrt{2\epsilon_L(1+\epsilon)} \frac{d\sigma_{TL}}{d\Omega_K} \right]$$

- $\Gamma$  and  $\epsilon$  are virtual photon flux factor and polarization, respectively,  $\epsilon_L = \epsilon Q^2/E_\gamma^2$ , and  $d\sigma/d\Omega_K$  are separated cross sections
- $d\sigma_T$  dominates due to very small  $Q^2 \leftrightarrow$  photoproduction ( $Q^2=0$ )
- $d\sigma_{TL}$  is important even for small  $Q^2$ :

the cross sections in  $^{12}\text{C}(e, e'K^+)^{12}\text{B}$  with  $Q^2 = 0.06 \text{ (GeV/c)}^2$

E	$J_H^P$	$\theta_{K\gamma}^{lab}$	$d\sigma$	$d\sigma_T$	$\epsilon_L d\sigma_L$	$\epsilon d\sigma_{TT}$	$\sqrt{2\epsilon_L(1+\epsilon)} d\sigma_{TL}$	$d^3\sigma$
0.0	1 <sup>-</sup>	1.8	36.768	42.505	0.251	0.040	-6.028	0.640
0.116	2 <sup>-</sup>	1.8	127.898	148.198	1.083	0.364	-21.747	2.227

- the transverse-longitudinal interference terms contribute more than 10%
- there is a difference between photo- and electroproduction calculations



# Formalism – the impulse approximation

- production by virtual photons:  $\gamma_v(q) + A(P_A) \rightarrow H(P_H) + K^+(P_K)$
- in IA the production goes on individual protons which is well justified for large momenta:  $|\vec{q}| \geq 1 \text{ GeV}/c \Rightarrow \lambda_B \leq 0.2 \text{ fm}$
- the many-particle matrix element

$$\langle \Psi_H | \sum_{i=1}^Z \mathcal{X}_\gamma \mathcal{X}_K^* \mathcal{J}_\mu^i(p_\Lambda, P_K, p_p^i, q) | \Psi_A \rangle$$

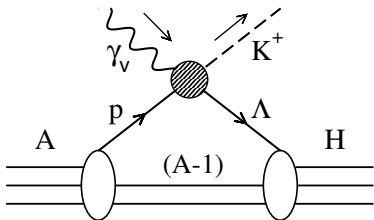
$\Psi_H, \Psi_A$  – hypernucleus and nucleus  
nonrelativistic wave functions

$\mathcal{J}_\mu^i$  – elementary production amplitude  
in two-component form

$\mathcal{X}_\gamma$  – photon plane wave

$\mathcal{X}_K$  – kaon distorted wave in eikonal approximation:

a good approximation as  $|\vec{P}_K| \approx 1 \text{ GeV}/c$  and the KN interaction is weak



## Formalism – the optimal factorization

- the elementary amplitude is integrated over the proton momentum  $\vec{p}_p$  in the many-particle matrix element
- assuming a constant **effective proton momentum** the elementary amplitude can be taken out of the integral and we get the hypernucleus-production amplitude in the **optimal-factorization approximation (OFA)**

$$\begin{aligned} \mathcal{T}_\mu &= Z \text{Tr} \left[ \mathcal{J}_\mu(\vec{P}_K, \vec{p}_{\text{eff}}, \vec{q}) \int d^3\xi e^{iB\vec{\Delta}\cdot\vec{\xi}} \mathcal{X}_K^*(\vec{p}_K, B\vec{\xi}) \right. \\ &\quad \left. \times \int d^3\xi_1 \dots d^3\xi_{A-2} \Phi_A(\vec{\xi}_1, \dots, \vec{\xi}_{A-2}, \vec{\xi}) \Phi_H^*(\vec{\xi}_1, \dots, \vec{\xi}_{A-2}, \vec{\xi}) \right] \end{aligned}$$

with still unspecified effective momentum  $\vec{p}_{\text{eff}}$ , the momentum transfer  $\vec{\Delta} = \vec{q} - \vec{P}_K$ , Jacobi coordinates  $\vec{\xi}$ , and  $B = (A - 1)/(A - 1 + m_\Lambda/m_p)$

- OFA is also used to describe the  $\pi$ ,  $p$ , and  $\bar{p}$  scattering off nuclei
- in previous calculations the “frozen-proton” approximation,  $\vec{p}_{\text{eff}} = 0$  was used as in the Lab frame the amplitude  $\mathcal{J}_j(\vec{P}_K, 0, \vec{q})$  has a simple two-component form – only six CGNL amplitudes  $F_i$ .

## Formalism – the elementary amplitude in a two-component form

- in many-particle calculations the elementary amplitude is rewritten

$$\mathcal{J} \cdot \varepsilon = \bar{u}_\Lambda(\mathbf{p}_\Lambda) \gamma_5 \left( \sum_{j=1}^6 \hat{M}_j \cdot \varepsilon A_j(s, t, Q^2) \right) u_p(\mathbf{p}_p) = X_\Lambda^+ (\vec{J} \cdot \vec{\varepsilon}) X_p$$

where  $\vec{J}$  has the two-component form and its time component was eliminated using  $\varepsilon_\mu = \varepsilon_\mu - \varepsilon_0 \mathbf{q}_\mu / q_0 = (0, \vec{\varepsilon})$ ;  $X_x$  are Pauli spinors,  $s = (\mathbf{q} + \mathbf{p}_p)^2$ ,  $t = (\mathbf{q} - \mathbf{p}_K)^2$

- a **general two-component form** has 16 terms

$$\vec{J} \cdot \vec{\varepsilon} = G_1 (\vec{\sigma} \cdot \vec{\varepsilon}) + G_2 i(\vec{p}_p \times \vec{q} \cdot \vec{\varepsilon}) + \dots G_{15} (\vec{\sigma} \cdot \vec{P}_K)(\vec{p}_p \cdot \vec{\varepsilon}) + G_{16} (\vec{\sigma} \cdot \vec{P}_K)(\vec{P}_K \cdot \vec{\varepsilon})$$

the CGLN-like amplitudes  $G_i$  are written via  $A_j$  and not all of them are independent

- in the special case:  $\vec{p}_p = 0$  (similarly in the c.m. frame,  $\vec{p}_p = -\vec{q}$ )

$$\begin{aligned} \vec{J}_{LAB} \cdot \vec{\varepsilon} = & G_1 (\vec{\sigma} \cdot \vec{\varepsilon}) + G_3 i(\vec{P}_K \times \vec{q} \cdot \vec{\varepsilon}) + G_8 (\vec{\sigma} \cdot \vec{q})(\vec{q} \cdot \vec{\varepsilon}) + \\ & G_{10} (\vec{\sigma} \cdot \vec{q})(\vec{P}_K \cdot \vec{\varepsilon}) + G_{14} (\vec{\sigma} \cdot \vec{P}_K)(\vec{q} \cdot \vec{\varepsilon}) + G_{16} (\vec{\sigma} \cdot \vec{P}_K)(\vec{P}_K \cdot \vec{\varepsilon}) \end{aligned}$$

- the general two-component form was already used by Mart et.al for  ${}^3\text{H}$  [Nucl. Phys. A 640, 235 (1998)]

## Formalism – the spherical amplitudes

- it is convenient to use the spherical components

$$\vec{J} \cdot \vec{\epsilon} = -\sqrt{3} [J^{(1)} \otimes \epsilon^{(1)}]^0 = \sum_{\lambda} (-1)^{-\lambda} J_{\lambda}^{(1)} \epsilon_{-\lambda}^{(1)} = \sum_{\lambda S \xi} (-1)^{-\lambda} \mathcal{F}_{\lambda \xi}^S \sigma_{\xi}^S \epsilon_{-\lambda}^{(1)}$$

where  $\mathcal{F}_{\lambda \xi}^S$  are the spherical amplitudes with  $S = 0, 1$  (spin non-flip and flip) and with projections  $\lambda$  (photon),  $\xi = \pm 1, 0$ ;  $\sigma_{\xi}^1$  are the spherical Pauli matrixes and  $\sigma^0 = 1$

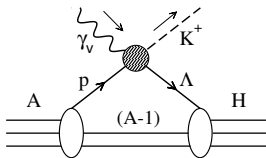
- then explicitly

$$\begin{aligned} \vec{J} \cdot \vec{\epsilon} = & - \epsilon_{-1}^1 ( \mathcal{F}_{-10}^0 + \sigma_1^1 \mathcal{F}_{-11}^1 + \sigma_0^1 \mathcal{F}_{-10}^1 + \sigma_{-1}^1 \mathcal{F}_{-1-1}^1 ) + \\ & + \epsilon_0^1 ( \mathcal{F}_{00}^0 + \sigma_1^1 \mathcal{F}_{01}^1 + \sigma_0^1 \mathcal{F}_{00}^1 + \sigma_{-1}^1 \mathcal{F}_{0-1}^1 ) - \\ & - \epsilon_{-1}^1 ( \mathcal{F}_{10}^0 + \sigma_1^1 \mathcal{F}_{11}^1 + \sigma_0^1 \mathcal{F}_{10}^1 + \sigma_{-1}^1 \mathcal{F}_{1-1}^1 ) \end{aligned}$$

- the spherical amplitudes  $\mathcal{F}_{\lambda \xi}^S$  are expressed via the CGLN-like amplitudes  $G_i$ .
- here we will use the elementary amplitudes:  
SLA [Phys. Rev. C **53**, 2613 (1996); **58**, 75 (1998)]  
BS3 [Phys. Rev. C **93**, 025204 (2016); **97**, 025202 (2018)]

## Formalism – the optimum on-shell approximation

- the general form of elementary amplitude allows to use “arbitrary”  $\vec{p}_{eff}$
- the assumptions:



- many-body energy-momentum conservation holds  $\rightarrow |\vec{P}_K|_{mb}$
- binding effects are neglected:  $e_p - e_\Lambda \approx 0$
- the **elementary amplitude is on-shell**:  
 $p$  and  $\Lambda$  are on-mass-shell and  $q + p_p = P_K + p_\Lambda$

- these assumptions can only be accomplished with a special “optimum” value of  $\vec{p}_{eff}$  where the magnitude of the **optimum momentum** satisfies

$$E_\gamma + \sqrt{m_p^2 + (\vec{p}_{opt})^2} = \sqrt{m_\Lambda^2 + |\vec{P}_K|_{mb}^2} + \sqrt{m_\Lambda^2 + (\vec{\Delta} - \vec{p}_{opt})^2}$$

with the momentum transfer  $\vec{\Delta} = \vec{q} - \vec{P}_K$ .  $|\vec{p}_{opt}|$  is not unique, it depends on  $\theta_{\Delta p}$ . Note that in calculations with frozen-proton ( $\vec{p}_{eff} = 0$ ) and on-shell elementary amplitude there are two values of kaon momentum  $|\vec{P}_K|_{mb} \neq |\vec{P}_K|_{2b}$ .

- one can fix  $|\vec{p}_{opt}| = p_{mean} = \sqrt{2\mu \langle T_{kin} \rangle}$  and determine  $\theta_{\Delta p}$

## Formalism – further details

- partial-wave decomposition:  $\mathcal{X}_K^* \mathcal{X}_\gamma = \sum F_{LM}(B|\vec{\xi}|, \vec{\Delta}) Y_{LM}(\hat{\xi})$   
where  $F_{LM}$  includes the spherical Bessel function in PWIA  
or a projected kaon distorted wave in DWIA
- the kaon distorted wave function in eikonal approximation with  $V_{\text{opt}}^{\text{1st}}$   
depends on  $\sigma_{KN}^{\text{tot}}$ ,  $\alpha_o = \text{Re } f^{KN}(0)/\text{Im } f^{KN}(0)$ , and nucleus density  $\rho(\vec{r})$ ;  
 $f^{KN}(0)$  is the isospin averaged forward angle amplitude from  
a separable model with partial waves  $\ell = 0, 1, \dots, 7$  ( $0 \leq E_{\text{kin}} \leq 2 \text{ GeV}$ );
- single-particle basis:  $|\alpha\rangle = |n \ell \frac{1}{2} j\rangle$
- the **many-particle structure** is included via reduced matrix elements of the  
single-particle operator (OBDME) ( $\Psi_H(J_H) || [b_{\alpha'}^+ \otimes a_\alpha]^J || \Psi_A(J_A)$ )  
obtained from the shell-model, Tamm-Dancoff,... calculations
- the radial part of the transition operator is given by **radial integrals**:  
$$\mathcal{R}_{\alpha'\alpha}^{LM} = \int_0^\infty dr r^2 R_{\alpha'}^* F_{LM} R_\alpha \quad \text{where } R_\alpha \text{ are the radial single-particle wave functions of p and } \Lambda \text{ (HO, Woods-Saxon, HF)}$$

## Formalism – the differential cross section

- it is suitable to introduce **reduced** (partial-wave) **amplitudes**:

$$\mathcal{T}_\lambda^{(1)} = \sum_{Jm} \frac{1}{[J_H]} C_{J_A M_A J m}^{J_H M_H} A_{Jm}^\lambda$$

which read as

$$A_{Jm}^\lambda = \frac{1}{[J]} \sum_{S\eta} \mathcal{F}_{\lambda\eta}^S \sum_{LM} C_{L M S \eta}^{J m} \sum_{\alpha'\alpha} \mathcal{R}_{\alpha'\alpha}^{LM} \mathcal{H}_{\ell'j'\ell j}^{LSJ} (\Psi_H \| [b_{\alpha'}^+ \otimes a_\alpha]^J \| \Psi_A)$$

- the transversal response function:

$$\frac{d\sigma_T}{d\Omega_K} = \frac{\beta}{2(2J_A + 1)} \sum_{Jm} \frac{1}{2J + 1} (|A_{Jm}^{+1}|^2 + |A_{Jm}^{-1}|^2)$$

- the longitudinal response function is given by the longitudinal component of the partial-wave amplitude:

$$\frac{d\sigma_L}{d\Omega_K} = \frac{\beta}{2J_A + 1} \sum_{Jm} \frac{1}{2J + 1} |A_{Jm}^0|^2$$

# Results – the proton Fermi motion in $^{12}\text{C}(\gamma_\nu, \text{K}^+)^{12}\text{B}$

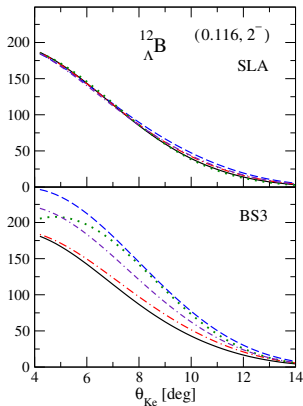
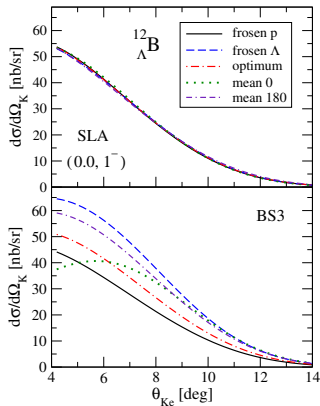
proton momentum:  $\vec{p}_{\text{eff}} = 0 \Rightarrow \vec{p}_\Lambda = \vec{q} - \vec{P}_K = \vec{\Delta}$  (frozen p)

$\vec{p}_{\text{eff}} = -\vec{\Delta} \Rightarrow \vec{p}_\Lambda = 0$  (frozen  $\Lambda$ )

$\vec{p}_{\text{eff}} = \vec{p}_{\text{opt}}$  with  $\theta_{\Delta p} = 180^\circ$  (optimum)

the mean momentum in  $^{12}\text{C}$ :  $|\vec{p}_{\text{eff}}| = \langle p \rangle = \sqrt{2\mu\langle T_{\text{kin}} \rangle}$

$|\vec{p}_{\text{eff}}| = 179 \text{ MeV}/c$  (0p orbit) with  $\theta_{p\gamma} = 0$  and  $180^\circ$



kinematics:

$E_\gamma = 2.2 \text{ GeV}$ ,

$Q^2 = 0.06 \text{ (GeV}/c)^2$

$|\vec{\Delta}| \in (240, 350) \text{ MeV}/c$

in optimum approximation

$|\vec{p}_{\text{opt}}| \in (94, 183) \text{ MeV}/c$

$|\vec{p}_\Lambda| \in (166, 265) \text{ MeV}/c$

OBDME from shell-model calculations by Millener with dominant transition

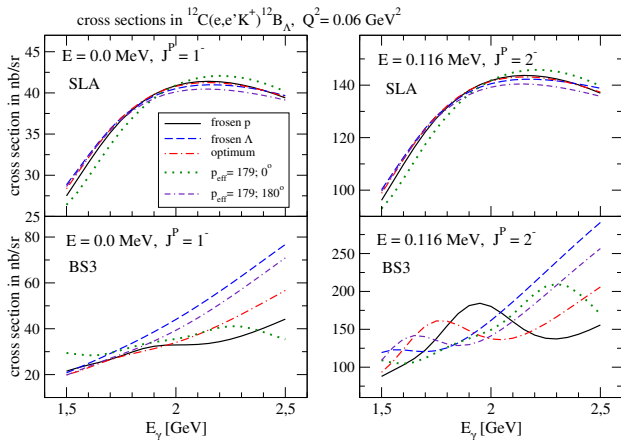
$0p_{3/2} \rightarrow 0s_\Lambda$

[P. B. et al, PHYSICAL REVIEW C 108, 024615 (2023)]

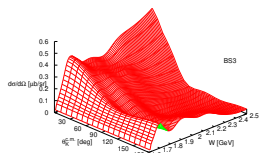
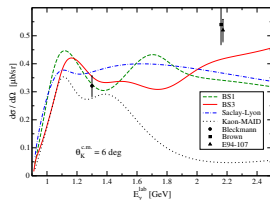


# Results – the proton Fermi motion effects

- a dependence on  $E_\gamma$  with  $Q^2 = 0.06$  (GeV/c)<sup>2</sup>,  $\varepsilon = 0.7$ ,  $\Phi_K = 180^\circ$ ,  $\theta_{Ke} = 6^\circ$
- the selection rule:  $A_{Jm}^0 \sim C_{1010}^{J_H 0} \Rightarrow$  the longitudinal contributions only for even  $J_H$
- the longitudinal contributions depend quite strongly on  $\vec{p}_{eff}$
- the effects depend on the elementary amplitude
  - $\rightarrow$  at  $E_\gamma > 2.2$  GeV BS3 predicts rising cross sections



rising cross sections with BS3

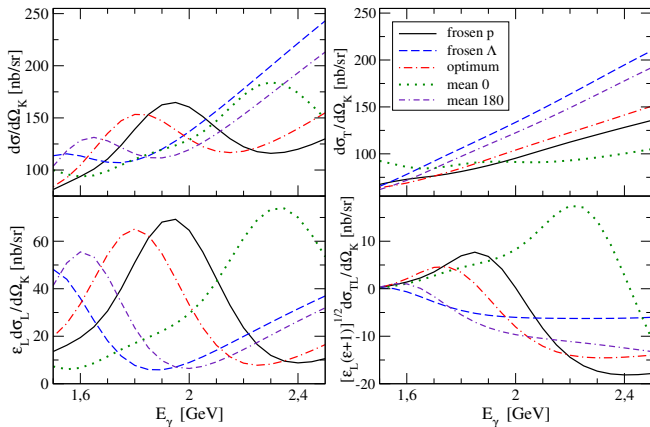


[D. Skoupil, P. B.,  
Phys. Rev. C 97 (2018) 025202]

# Results – the proton Fermi motion

the separated cross sections for the excited state ( $11.132, 3^+$ ) of  ${}^{12}_{\Lambda}\text{B}$

- the longitudinal part of the reduced amplitude contributes:  $A_{30}^0 \sim C_{2010}^{30} = \sqrt{3/5}$
- $d\sigma_L$  and  $d\sigma_{TL}$  are important making the difference between photoproduction ( $d\sigma_T$ ) and electroproduction ( $d\sigma$ ) results even at a small photon virtuality,  $Q^2 = 0.06 \text{ GeV}^2$



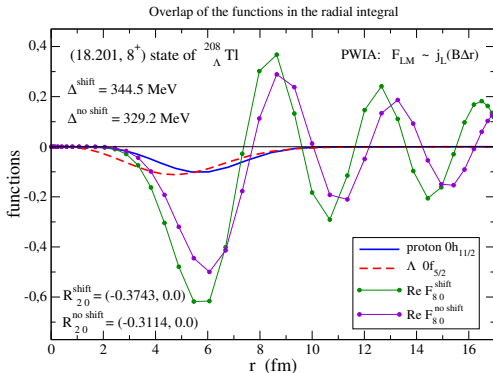
Fermi motion effects

- very important in  $d\sigma_L$  and  $d\sigma_{TL}$
- depend on  $|\vec{p}_{eff}|$  and elementary amplitude

# Results – mass effects in the cross sections of $^{208}_{\Lambda}\text{Tl}$

- an uncertainty in the ground state hypernucleus mass  $M_H^0$  (the binding energy)
- considering a shift of the hypernucleus mass due to excitation:  $M_H^* = M_H^0 + E^*$   
 $\Rightarrow |\vec{P}_K|, |\vec{\Delta}|, |\vec{p}_{opt}|, \mathcal{F}_{\lambda\eta}^S$  and  $\mathcal{R}_{\alpha'\alpha}^{LM}$  depend on  $E^*$
- effects of the mass shift in the states ( $E^*[\text{MeV}], J^P$ ) of  $^{208}_{\Lambda}\text{Tl}$   
 (PWIA,  $\text{TD}_{\Lambda}$ , Nijmegen F YNG,  $E_{\gamma} = 1.5 \text{ GeV}$ ,  $Q^2 = 0.0383 \text{ GeV}^2$ ,  $\theta_K = 8^\circ$ )

	(11.964, $8^-$ )	(18.201, $8^+$ )
$M_H$	0.006%	0.009%
$ \vec{P}_K $	-1.0%	-1.6%
$ \vec{\Delta} $	3.0%	4.6%
$ \vec{p}_{opt} $	-15.7%	-23.5%
$\text{Re}\mathcal{F}_{00}^1$	-1.2%	-4.5%
$\text{Im}\mathcal{F}_{00}^1$	-31.4%	-44.4%
$\mathcal{R}_{\alpha'\alpha}^{LM}$	$\mathcal{R}_{\alpha'\alpha}^{70} : -3.7\%$	$\mathcal{R}_{\alpha'\alpha}^{80} : 20.2\%$
	$0h_{11/2} \rightarrow 0d_{5/2}$	$0h_{11/2} \rightarrow 0f_{5/2}$
$d\sigma$	-16.0%	-10.6%
$d\sigma_T$	-13.2%	-9.6%



## Results – effects from kaon distortion in $^{12}_{\Lambda}\text{B}$

- comparison of PWIA and DWIA cross sections:  $\text{diff} = 100 \cdot (\text{PWIA} - \text{DWIA}) / \text{PWIA}$  in kinematics of the E94-107 JLab experiment,  $E_{\gamma} = 2.21$  GeV,  $|\vec{P}_K| = 1.96$  GeV, and  $\theta_K = 1.8^{\circ}$  with the KN scattering at  $W_{KN} = 2.2$  GeV and  $\sigma_{KN}^{\text{tot}} = 17.83$  mb
- differences are 35(higher states)–45(lower states)% similarly in SM and  $\text{TD}_{\Lambda}$ , except the state **(11.542,  $1^{+}$ )** where the leading contributions  $0p_{3/2} \rightarrow 0p_{1/2}$  and  $0p_{3/2} \rightarrow 0p_{3/2}$  compose themselves together, opposite to the case of the weakly populated state **(10.706,  $1^{+}$ )** where the relative phase is negative (the phase is given by the sign at the OBDME and the radial integral)

cross sections in $\text{TD}_{\Lambda}$					cross sections in SM				
energy	$J^P$	PWIA	DWIA	diff	energy	$J^P$	PWIA	DWIA	diff
MeV		nb/sr	nb/sr	%	MeV		nb/sr	nb/sr	%
0.000	$1^{-}$	126.97	70.34	45	0.000	$1^{-}$	74.14	41.65	44
0.060	$2^{-}$	406.68	224.63	45	0.116	$2^{-}$	268.38	150.10	44
10.667	$2^{+}$	107.46	69.30	36	10.480	$2^{+}$	17.11	11.09	35
<b>10.706</b>	$1^{+}$	13.11	8.25	37	10.525	$1^{+}$	8.89	5.53	38
10.845	$2^{+}$	63.27	40.71	36	11.059	$2^{+}$	84.63	54.66	35
10.986	$3^{+}$	286.20	187.23	35	11.132	$3^{+}$	179.72	117.85	34
<b>11.542</b>	$1^{+}$	1.17	3.58	<b>-205</b>	11.674	$1^{+}$	2.34	4.72	<b>-102</b>

# Results – effects from kaon distortion in ${}_{\Lambda}^{48}\text{K}$

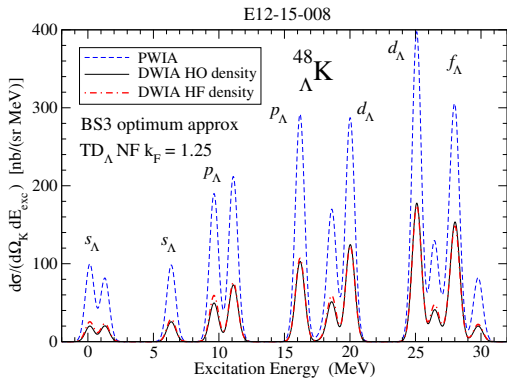
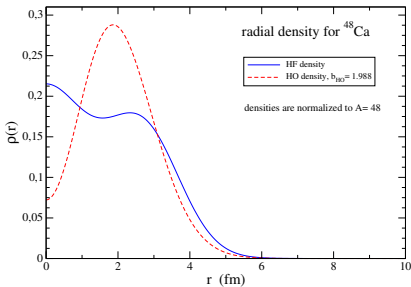
- the kaon-nucleus optical potential

$$V_{\text{opt}}^{\text{1st}}(\vec{r}) = -\beta \sigma_{KN}^{\text{tot}}(s) \frac{1}{2} [i + \alpha(s)] \rho(\vec{r})$$

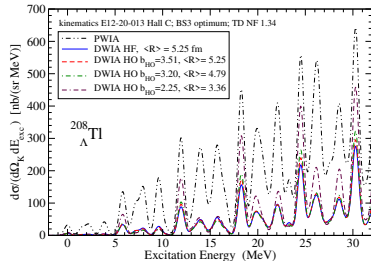
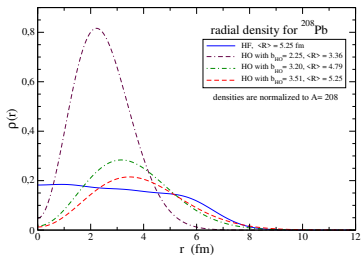
- the kaon distorted wave function in eikonal approximation

$$\chi^*(\vec{r}) = \exp \left[ -i\vec{P}_K \cdot \vec{r} - b \sigma_{KN}^{\text{tot}} (1 - i\alpha) \int_0^\infty dt \rho(\vec{r} + \hat{p}t) \right]$$

- distortion is 50–60% and depends mainly on behavior of  $\rho(\vec{r})$  in the peripheral region



# Results – effects from kaon distortion in $^{208}_{\Lambda}\text{Tl}$ are $\approx 50\text{--}90\%$



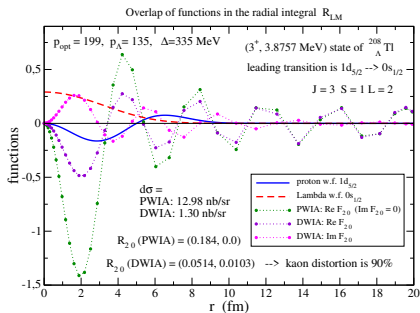
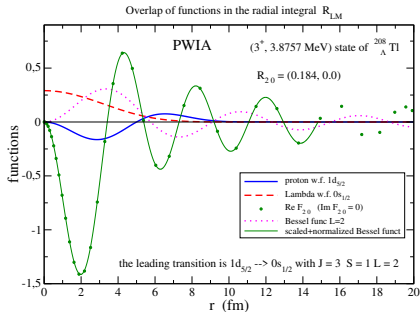
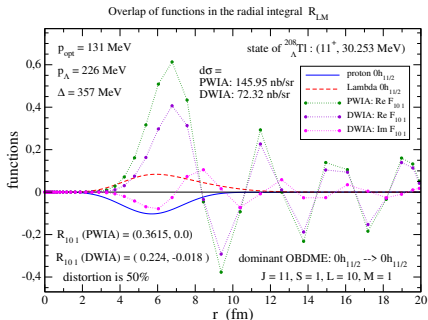
$E^*, J^P$	$l_{\Lambda}$	cross sections in nb/sr				
		PWIA	DWIA HO	diff %	DWIA HF	diff %
0.000, $6^-$	$s_{\Lambda}$	11.96	1.88	84	2.07	82
3.857, $3^+$	$s_{\Lambda}$	12.67	1.17	90	1.26	90
5.794, $6^+$	$p_{\Lambda}$	25.34	5.13	79	5.05	80
5.804, $7^+$	$p_{\Lambda}$	52.81	11.73	77	11.69	77
7.955, $2^-$	$p_{\Lambda}$	27.72	3.15	88	3.51	87
7.969, $3^-$	$p_{\Lambda}$	34.79	4.44	87	5.00	85
11.964, $8^-$	$d_{\Lambda}$	111.26	33.27	70	30.93	72
13.705, $4^-$	$p_{\Lambda}$	22.49	2.75	87	3.11	86
13.720, $5^-$	$p_{\Lambda}$	24.36	3.82	84	4.10	83
15.692, $5^+$	$d_{\Lambda}$	91.79	14.42	84	16.12	82
18.201, $8^+$	$f_{\Lambda}$	86.00	28.09	67	25.52	70
20.286, $3^+$	$p_{\Lambda}$	11.01	1.01	90	1.07	90
21.685, $2^-$	$p_{\Lambda}$	42.57	7.24	82	7.72	81
22.034, $6^-$	$f_{\Lambda}$	81.52	17.95	77	18.87	76
24.453, $7^-$	$g_{\Lambda}$	28.05	7.25	74	6.59	76
24.472, $9^-$	$g_{\Lambda}$	92.66	36.96	60	33.19	64
26.220, $7^-$	$f_{\Lambda}$	78.46	20.99	73	19.94	74
28.673, $8^-$	$f_{\Lambda}$	106.61	27.27	74	25.85	75
29.343, $5^+$	$d_{\Lambda}$	73.59	14.43	80	15.99	78
30.246, $9^+$	$h_{\Lambda}$	36.21	12.56	65	10.86	70
30.253, $11^+$	$h_{\Lambda}$	147.78	79.76	46	73.71	50
32.361, $7^+$	$g_{\Lambda}$	101.38	29.12	71	26.52	73
32.443, $8^+$	$g_{\Lambda}$	81.60	28.02	65	25.54	68

# Results – kaon distortion

the different effects are due to the radial integral:

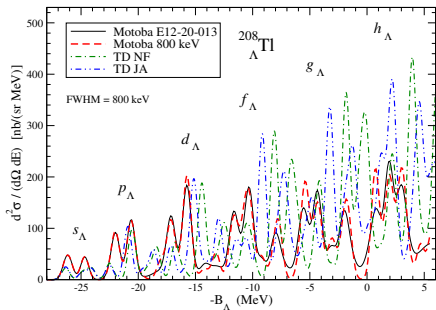
$$\mathcal{R}_{\alpha'\alpha}^{LM} = \int_0^\infty dr r^2 R_{\alpha'}^* F_{LM} R_\alpha$$

real in PWIA and complex in DWIA

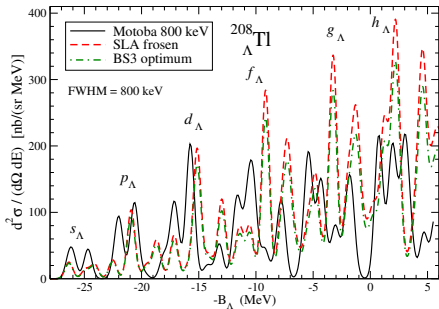


# Results – effects from the nucleus-hypernucleus structure

- Tamm-Dancoff self-consistent many-body calculations using the NN Daejeon16 interaction with a phenomenological density dependent (DD) term and **effective YN interactions**;
- the effective YN interactions: Nijmegen-F and Jülich A YNG with  $k_F = 1.34$  fm
- kinematics:  $E_\gamma = 1.5$  GeV,  $Q^2 = 0.012$  GeV<sup>2</sup>,  $|\vec{P}_K| = 1.176$  GeV,  $\theta_K = 0.5^\circ$
- the rising background in TD<sub>Λ</sub> is due to many weakly populated states
- the result by Motoba and Millener are from the proposal of the JLab experiment E12-20-013



different YNG interactions  
with the SLA amplitude

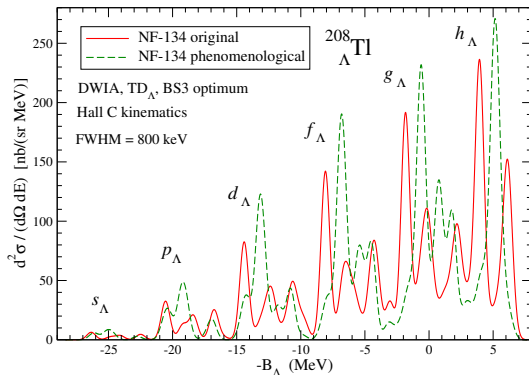
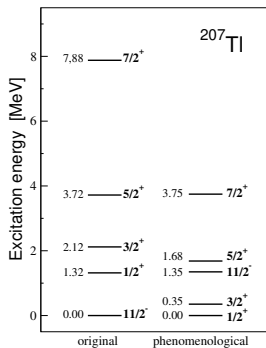


different elementary amplitudes  
with the Jülich A YNG interaction



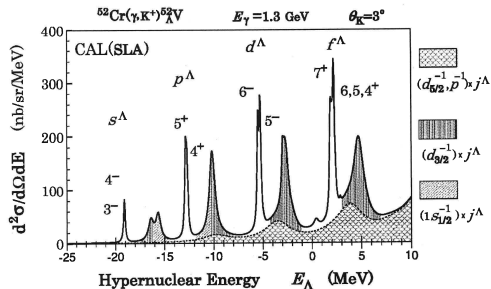
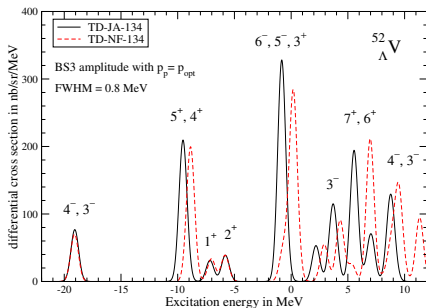
# Results – tuning the nucleus structure

- nucleus is described as a core-particle system:  $|^{208}\text{Pb}_{g.s.}\rangle = \sum |^{207}\text{Tl}(E_c, J_c^{P_c})\rangle \otimes |(n l j)_p\rangle$
- similarly hypernucleus:  $|^{208}_{\Lambda}\text{Tl}(E_H, J_H^{P_H})\rangle = \sum |^{207}\text{Tl}(E_c, J_c^{P_c})\rangle \otimes |(n' l' j')_{\Lambda}\rangle$
- the core nucleus is a “spectator” in the impulse approximation
- spectrum of the core nucleus calculated in  $\text{TD}_{\Lambda}$  with the NN Daejeon16 interaction and the DD term (original) is modified introducing phenomenological energies
- modification of the  $^{208}_{\Lambda}\text{Tl}$  excitation spectrum



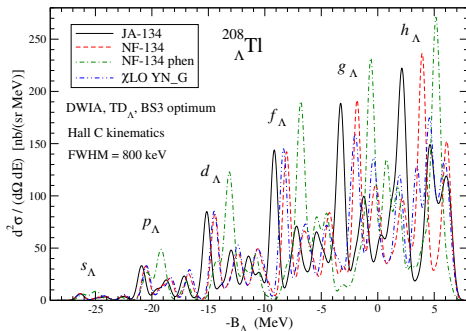
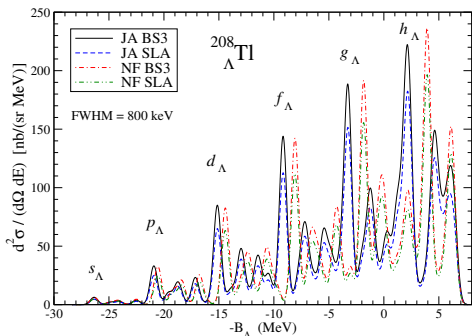
# Results – electroproduction of ${}_{\Lambda}^{52}\text{V}$

- the excitation spectrum in  ${}^{52}\text{Cr}(e,e'\text{K}^+){}_{\Lambda}^{52}\text{V}$
- the NN Daejeon16 interaction with the phenomenological density dependent term
- the Nijmegen-F and Jülich A YNG interaction with  $k_F = 1.34$  fm
- the BS3 amplitude in the optimum on-shell approximation
- kinematics:  $E_{\gamma} = 1.3$  GeV,  $Q^2 = 0.003$  GeV<sup>2</sup>, and  $\theta_K = 3^{\circ}$
- comparison with older results from P.B., M.Sotona, T.Motoba, K.Itonaga, K.Ogawa, and O.Hashimoto, Nuc. Phys. **881**, 199 (2012).



# Results – predictions for the E12-20-013 experiment at JLab

- the reaction:  $^{208}\text{Pb}(e,e'\text{K}^+)^{208}_{\Lambda}\text{Tl}$
- the many-particle calculation: the Tamm-Dancoff  $\Lambda$ -nucleon particle-hole model
- the NN interaction: Daejeon16 with the phenomenological density dependent term
- the YNG interaction: Nijmegen-F and Jülich A with  $k_F = 1.34$  fm
- Hall C kinematics:  $E_\gamma = 1.5$  GeV,  $Q^2 = 0.0323$  GeV<sup>2</sup>,  $|\vec{P}_K| = 1.245$  GeV,  $\theta_K = 7.1^\circ$ ,  $\Phi_K = 180^\circ$

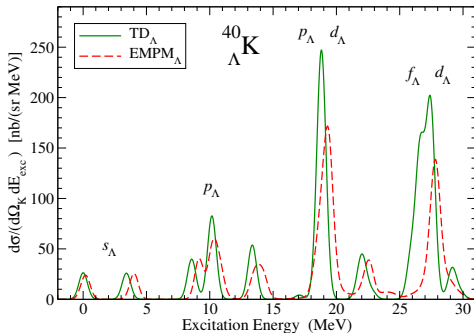
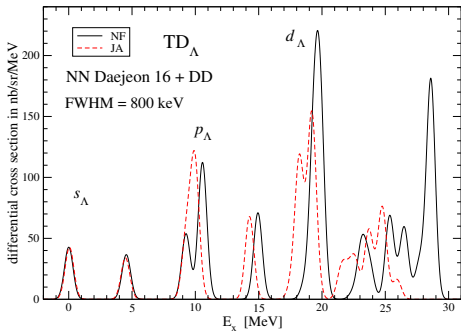


# Results – predictions for the E12-15-008 experiment at JLab

- the reaction:  $^{40}\text{Ca}(e,e'K^+)^{40}\Lambda\text{K}$
- the many-particle calculation: the Tamm-Dancoff  $\Lambda$ -nucleon particle-hole model
- the NN interaction: chiral NNLO<sub>sat</sub> NN+NNN as in Phys.Rev.C **108**, 024615 (2023) and Daejeon 16 with the phenomenological density dependent term
- the YNG interaction: Nijmegen-F and Jülich A with  $k_F = 1.30$  fm
- kinematics:  $E_\gamma = 1.5$  GeV,  $Q^2 = 0.0323$  GeV<sup>2</sup>,  $|\vec{P}_K| = 1.245$  GeV,  $\theta_K = 7.1^\circ$ ,  $\Phi_K = 180^\circ$
- BS3 amplitude in the optimum on-shell approximation

Excitation spectrum of  $^{40}\Lambda\text{K}$

DWIA calculations with BS3 and kinematics E12-15-008

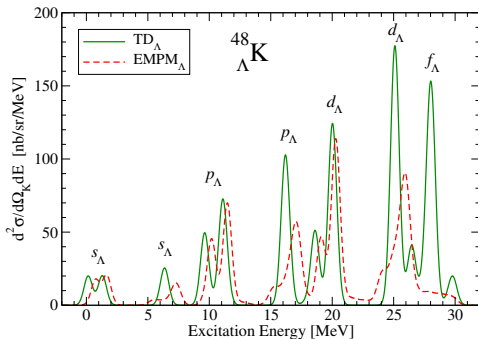
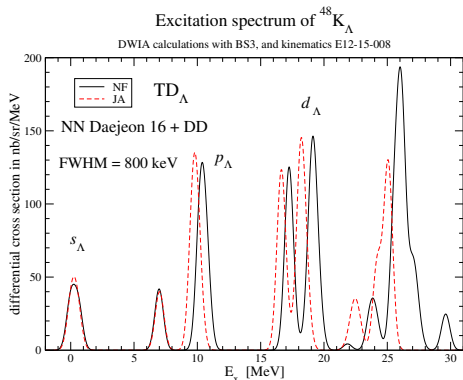


Phys. Rev. C **108**, 024615 (2023)



# Results – predictions for the E12-15-008 experiment at JLab

- the reaction:  $^{48}\text{Ca}(e,e'\text{K}^+)^{48}\text{K}_\Lambda$
- the many-particle calculation: the Tamm-Dancoff  $\Lambda$ -nucleon particle-hole model
- the NN interaction: chiral NNLO<sub>sat</sub> NN+NNN as in Phys.Rev.C **108**, 024615 (2023) and Daejeon 16 with the phenomenological density dependent term
- the YNG interaction: Nijmegen-F and Jülich A with  $k_F = 1.34$  fm
- kinematics:  $E_\gamma = 1.5$  GeV,  $Q^2 = 0.0323$  GeV<sup>2</sup>,  $|\vec{P}_K| = 1.245$  GeV,  $\theta_K = 7.1^\circ$ ,  $\Phi_K = 180^\circ$



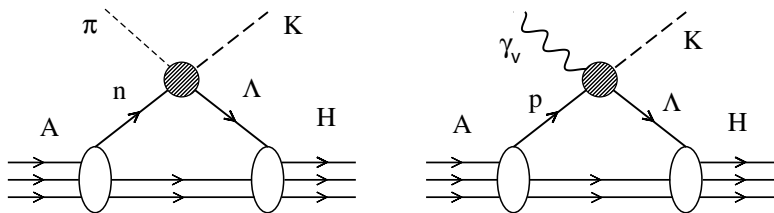
Phys. Rev. C **108**, 024615 (2023)

# Summary

- the effects from proton Fermi motion in electroproduction of hypernuclei depend on the elementary amplitude and kinematics and they are more apparent in the longitudinal parts of the cross section
- we have suggested using the optimum on-shell approximation that effectively accounts for the proton motion and improves agreement with the data
- the shell-model approach with the effective YN interaction fitted to very precise data from the  $\gamma$ -ray spectroscopy provide reasonable description of spectra in electroproduction of p-shell (light) hypernuclei
- Tamm-Dancoff formalism with the chiral NNLO<sub>sat</sub> NN+NNN potential and Daejeon 16 with the phenomenological DD term and various effective YN interactions (Nijmegen, Jülich) turn out to be a good tool in analysis of the data in electroproduction of medium ( ${}^{40}_{\Lambda}\text{K}$ ) and heavy ( ${}^{208}_{\Lambda}\text{Tl}$ ) mass hypernuclei
- we provided predictions for the experiments in preparation at JLab
- correct inclusion of kaon distortion is important as in given kinematics the distortion amounts to  $\approx 30\text{--}40\%$  for light (p-shell) and  $\approx 50\text{--}90\%$  for heavy hypernuclei

# Outlook

- include Coulomb interaction in the kaon FSI ( $Z = 81$  for  ${}^{208}_{\Lambda}\text{Tl}$ )
- a more ambitious project: develop analogous formalism for  $(\pi^+, K^+)$  production and utilize consistent calculations of the many-particle part (OBDME)



Thank you for your attention!



## Backup slide – factorization

- production amplitude in PWIA

$$\mathcal{T}_j = Z \int d^3 \xi_\Lambda d^3 \xi_p e^{iB\vec{\Delta} \cdot \vec{\xi}_\Lambda} \text{Tr} \int \frac{d^3 p_p}{(2\pi)^3} \exp \left[ i \vec{p}_p \cdot (\vec{\xi}_\Lambda - \vec{\xi}_p) \right] \mathcal{J}_j(\vec{P}_K, \vec{P}_\gamma, \vec{p}_p) \\ \int d^3 \xi_1 \dots d^3 \xi_{A-2} \Phi_A(\vec{\xi}_1, \dots, \vec{\xi}_{A-2}, \vec{\xi}_p) \Phi_H^*(\vec{\xi}_1, \dots, \vec{\xi}_{A-2}, \vec{\xi}_\Lambda),$$

with the momentum transfer  $\vec{\Delta} = \vec{P}_\gamma - \vec{P}_K$ , Jacobi coordinates  $\vec{\xi}$ , a scaling parameter  $B$  and assuming translational invariance

$$\langle \vec{P}_K \vec{p}_\Lambda | \hat{J}_j | \vec{P}_\gamma \vec{p}_p \rangle = (2\pi)^3 \delta^{(3)}(\vec{P}_K + \vec{p}_\Lambda - \vec{P}_\gamma - \vec{p}_p) \mathcal{J}_j(\vec{P}_K, \vec{P}_\gamma, \vec{p}_p).$$

– the amplitude is still averaged over the proton momentum  $\vec{p}_p$ .

– the elementary amplitude  $\mathcal{J}_j$  is a matrix  $2 \times 2$

(in two-component CGLN-like formalism)

- elementary amplitude is factorized out of the integral replacing  $\mathcal{J}_\mu(\vec{P}_K, \vec{P}_\gamma, \vec{p}_p) \rightarrow \mathcal{J}_\mu(\vec{P}_K, \vec{P}_\gamma, \vec{p}_{eff})$  for some (unknown) effective proton momentum  $\vec{p}_{eff}$ .

## Backup slide – effective proton momentum

- another possibility how to fix  $p_{eff}$  is to use a **mean value** calculated from the mean kinetic energy of the proton in nucleus

$$\langle T_{kin} \rangle = \frac{\langle p \rangle^2}{2\mu} \Rightarrow \langle p \rangle = \sqrt{2\mu \langle T_{kin} \rangle} = |\vec{p}_{eff}| \quad \text{where}$$

$$\begin{aligned} \langle \Psi_{Eljm} | T_{kin} | \Psi_{Eljm} \rangle &= \int dr u_{Elj}^*(r) \left( -\frac{(\hbar c)^2}{2\mu} \right) \left[ \frac{d^2}{dr^2} - \frac{l(l+1)}{r^2} \right] u_{Elj}(r) \\ &= \int dr |u_{Elj}(r)|^2 (E - \langle ljm | V | ljm \rangle) \end{aligned}$$

with the Woods-Saxon and Coulomb potentials:  $V = WS_c + WS_{LS} + V_{coul}$   
and the single-particle state:  $\Psi_{Eljm}(\vec{r}) = \frac{u_{Elj}(r)}{r} [Y_l(\hat{r}) \otimes \chi^{(\frac{1}{2})}] j_m$

- for the  $^{12}\text{C}$  target we get results:

proton state	E[MeV]	$WS_c$	$WS_{LS}$	$\langle T \rangle$	$\langle p \rangle$
$p_{1/2}$	-10.37	-54.18	18.98	18.16	<b>176.7</b>
$p_{3/2}$	-15.96	-54.18	-9.49	18.76	<b>179.6</b>

# Backup slide – off-shell effects

$^{12}\text{C}(e,e'\text{K}^+)^{12}\text{B}_\Lambda$  in frozen proton approximation

